ELSEVIER

Journal of Organometallic Chemistry 483 (1994) 77–89

Journal of Organometallic Chemistry

Structural and NMR spectroscopic characterization of η^3-Benzyl palladium(II) complexes

Giuseppe Gatti [a], José A. López [b], Carlo Mealli [b], Alfredo Musco [c,*]

[a] *Bruker Spectrospin SRL, Via G. Pascoli 70, 20133 Milano, Italy*

[b] *Istituto per lo Studio della Stereochimica ed Energetica dei Composti di Coordinazione (ISSECC, CNR), Via J. Nardi 39, 50132 Firenze, Italy*

[c] *Istituto di Scienze Chimiche, Università degli Studi di Urbino, 61029 Urbino, Italy*

Received 17 January 1994

Abstract

η^3-Benzyl palladium complexes have been prepared by insertion of styrene in the Pd–Me bond of the solvated cation $[L_2PdMe(solv)]^+$ (L_2 = chelating ligand). The η^3 coordination of the benzyl ligand has been elucidated by X-ray structure determination and NMR spectroscopy. NMR studies have shown that $[(\eta^3\text{-R-}\alpha\text{-benzyl})PdL_2]^+$ (R = Me or Et) undergo two dynamic processes in solution: $\eta^3 - \eta^1$ coordination of the benzyl group and ligand exchange of coordination sites. The TMEDA and DIPY complexes undergo a rapid and reversible reaction with carbon monoxide to yield $(R\text{-}\alpha\text{-benzylCO})PdL_2CO]^+$.

Keywords: η^3-Benzyl; Palladium(II); X-ray structure; NMR

1. Introduction

Coordination of the benzyl group to a transition metal may range from η^1 to η^5 [1]. The η^3 bonding is usually found in the late-transition-metal complexes [2]. Preparative methods of these complexes include protonation of coordinated styrene, styrene insertion into a metal–hydrogen bond and oxidative addition of benzyl halides followed by displacement of the coordinating anion. Here we report that insertion of styrene in the palladium methyl bond of coordinatively unsaturated cationic species is a viable route to the preparation of η^3-benzyl palladium complexes. The coordination mode of the benzyl group has been elucidated by X-ray structure determination and NMR studies. Preliminary data concerning the complexes and styrene-carbon monoxide alternating copolymerization are also presented.

2. Results and discussion

2.1. Synthesis of the complexes

Insertion of styrene into the Pd–Me bond of the solvated cation of complex **3** is a simple route to the synthesis of η^3-benzyl palladium complexes (Eq. (1)).

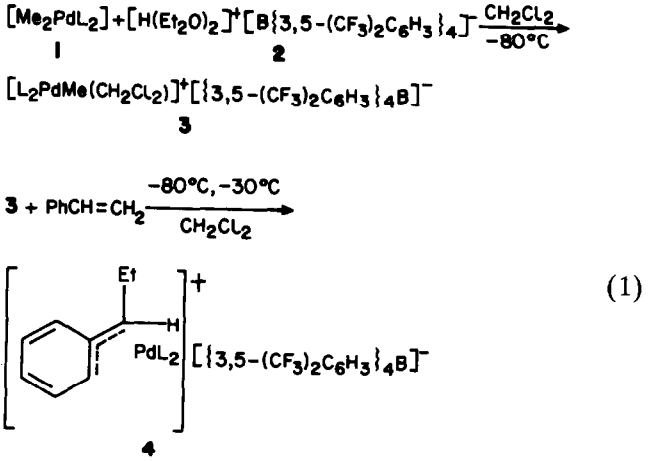

(1)

* Corresponding author.

SSDI 0022-328X(94)24689-G

Complexes **3** are easily prepared in methylene chloride by reaction of either $[Me_2PdTMEDA]$ [3] (**1a**, TMEDA = *N,N,N',N'*-tetramethylethylenediamine) or $[Me_2PdDIPY]$ [3] (**1b**, DIPY = 2,2'-dipyridyl) with stoichiometric amounts of tetrakis[3,5-bis(trifluoromethyl)-phenyl]boric acid (**2**). Preparation of **3** in acetonitrile has been previously reported [4], as well as the use of acid **2** to prepare soluble ionic complexes with a non-coordinating anion [5,6].

The protonation reaction of **1** was performed in methylene chloride at −80°C in the presence of an excess of styrene. On slowly raising the temperature from −80°C to −30°C a quantitative insertion of styrene in the Pd–Me bond takes place. Evaporation of the solvent in high vacuum at −30°C gave an oily residue which on scratching with a spatula yielded complex **4** as a yellow brown powder. While complex **4a** was obtained quantitatively, complex **4b** was contaminated by large amounts of complex **6b** (**4b**/**6b** ≈ 1:1) (Eq. (2)).

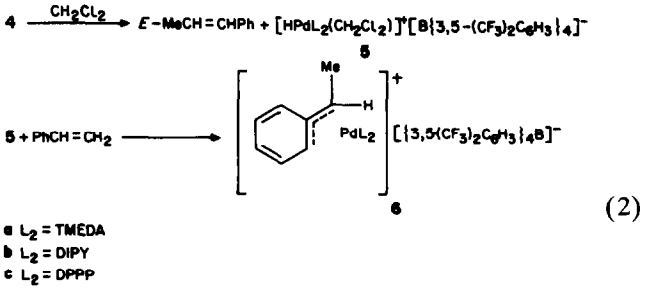

(2)

a L_2 = TMEDA
b L_2 = DIPY
c L_2 = DPPP

Complex **6b** is probably formed through styrene insertion in a Pd hydride species **5** derived from **4b** through β-hydrogen elimination. Indeed, *E*-α-methylstyrene has been identified in the reaction medium, which implies a stereoselective β-hydrogen elimination from complex **4b**. A quantitative transformation of **4b** into **6b** is achieved by keeping the reaction mixture at −10°C overnight. Transformation of **4a** into **6a** takes place at 25–50°C in methylene chloride and in the presence of an excess of styrene. Moreover, we have found that the reaction time may change from sample to sample, which suggests that the rate of β-hydrogen elimination from **4a** may be affected by impurities. It is known that solutions of **2** are unstable at room temperature, yielding $[3,5\text{-}(CF_3)_2C_6H_3]_3B$ [5]. We observed reproducible reaction times (8 h) if methylene chloride solutions of **4a** (0.05 M) containing an excess of styrene were warmed in presence of catalytic quantities of **2**. The reaction mechanism has not yet been investigated.

The TMEDA of **4a** is easily displaced by 1,3-bis(diphenylphosphino)-propane (DPPP) in methylene chloride at room temperature to yield quantitatively **4c** (Eq. (3)).

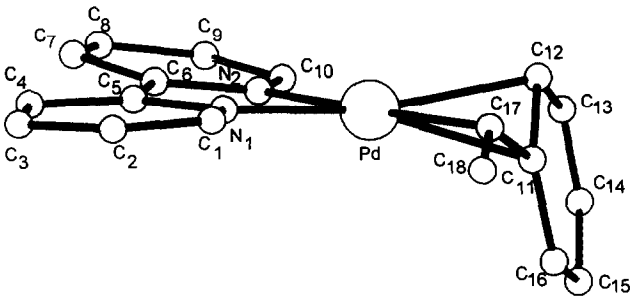

Fig. 1. A drawing of the cation complex $[(\eta^3\text{-}syn\text{-}\alpha\text{-methylbenzyl})Pd(dipy)]^+$ in complex (**6b**).

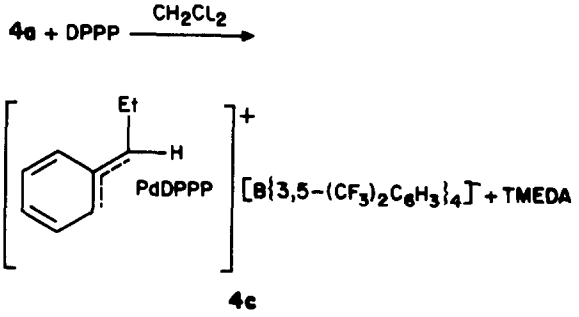

(3)

As with **4a**, complex **6c** and *E*-α-methylstyrene were obtained on warming chloroform solutions of **4c** in presence of an excess of styrene and catalytic amounts of 2 (Eq. (2)).

2.2. X-ray structure determination of $[(\eta^3\text{-}syn\text{-}\alpha\text{-methylbenzyl})Pd(dipy)]^+[B\{3,5\text{-}(CF_3)_2C_6H_3\}_4]^-$ (6b)

Fig. 1 shows a drawing of the complex cation $[(\eta^3\text{-}syn\text{-}\alpha\text{-methylbenzyl})Pd(dipy)]^+$. Selected bond distances and angles are collected in Table 1. As reported in the Experimental Section, the structure is affected by disorder mainly at the CF_3 groups of the anion, which reduces the overall quality of the crystallographic results. Nevertheless some features of chemical

Table 1
Selected bond distances (Å) and angles (°) of $[(\eta^3\text{-}syn\text{-}\alpha\text{-methylbenzyl})Pd(dipy)]^+$ (**6b**)

Pd–N(1)	2.06(1)	C(11)–C(12)	1.45(2)
Pd–N(2)	2.12(1)	C(13)–C(14)	1.15(4)
Pd–C(12)	2.28(2)	C(14)–C(15)	1.33(4)
Pd–C(17)	2.08(2)	C(15)–C(16)	1.40(4)
Pd–C(11)	2.13(1)	C(11)–C(17)	1.40(3)
C(12)–C(13)	1.46(3)	C(11)–C(16)	1.35(3)
C(17)–C(18)	1.25(3)		
N(1)–Pd–N(2)	77.2(5)	N(1)–Pd–C(11)	142.7(6)
N(1)–Pd–C(12)	167.4(7)	N(1)–Pd–C(17)	107.2(6)
N(2)–Pd–C(11)	136.8(6)	N(2)–Pd–C(12)	107.8(6)
N(2)–Pd–C(17)	174.9(6)	C(11)–Pd–C(12)	38.3(7)
C(11)–Pd–C(17)	38.8(7)	C(12)–Pd–C(17)	67.1(7)
C(12)–Pd–C(17)	116(2)		

significance are worth discussing. The structure is similar to that of a Pt analogue, $[(\eta^3\text{-}anti\text{-}1MeCHC_6H_4Br)Pt(Bu^t_2P(CH_2)_3PBu^t_2)]^+[BF_4]^-$ [2], in which the L_2Pt fragment is η^3-coordinated to the benzyl. The main difference in our case is the *syn* arrangement of the methyl group. The 2,2′-dipyridyl is affected by a minor torsion (ca. 7°) about the bond connecting the two six-membered rings and the coordination about the metal atom is essentially planar if the central allyl C_c atom (C11) is neglected. Indeed the inclination of the C3 plane (atoms C12, C11 and C17) to the square coordination plane at the metal is ca. 107°, close to the 110° value typical of η^3 allyl Pd and Pt complexes. In the case of normal allyl ligands, the 110° bending of the C3 plane allows the M–C_c distance to match the two M–C_t ones (C_t are the terminal atoms). In the present case, the Pd–C12 distance of 2.28(2) Å (C12 is the C_t atom belonging to the C6 ring) is significantly longer than the other Pd–C_c and Pd–C_t bonds of 2.13(1) and 2.08(2) Å, respectively. The weak link between Pd and the aryl carbon atoms are probably imposed by the inability of the benzyl to deform from overall planarity.

In a previous paper [7], we pointed out that the interactions between frontier allyl and metal orbitals are improved by the loss of planarity of the allyl upon η^3-coordination. This feature, already noted and quantified by other authors [8], was expressed by us in terms of a complex reorientation of the terminal C_tH_2 groups with respect to the coordinated C3 plane. Moreover the C_cH link is bent toward the metal by ca. 15°. Since in the present case, two allyl substituents (at one C_t and at the C_c atoms, respectively) are part of the rigid aromatic ring, the deformation capability of the allyl itself is strongly reduced. Only the exocyclic C_tHMe group (centred at C17) is flexible enough, and reorients to maximize the overlap between the carbon σ-hybrid and the appropriate metal orbital. The same cannot occur at C12 while the C11–C16 link is bent toward the metal by only 8°. The last gross structural features imply that for the Pd–C bond strengths decrease in the order Pd–C17 > Pd-C11 > Pd-C12.

2.3. NMR characterization

The 1D and 2D spectra of complexes **4** and **6** were obtained to elucidate structure and dynamics in solution. The ^{13}C spectra were assigned by heteronuclear inverse correlation 2D experiments. Homonuclear COSY experiments and in some cases 1D spectrum simulation provided full assignment of the ^1H spectra. From the values of the J scalar couplings and from the intensity of the cross peaks in 2D-NOESY spectra it was possible to infer the conformational structures in solution and to detect the exchange processes. The 2D-NOESY spectra were measured in the phase-sensitive mode in order to discriminate between positive and negative cross peaks, i.e. same sign and opposite sign relative to the diagonal peaks. It is known that in extreme narrowing conditions the positive peaks are due to transfer of magnetization through chemical exchange (ECSY correlation) whereas negative peaks are due to transfer through dipolar interaction (NOESY correlation). In addition, it has to be pointed out that if a nucleus A is dipolar coupled to a nucleus B which in turn is chemically exchanging with a third nucleus C one can expect an *indirect* NOE effect between A and C besides the *direct* NOE effect between A and B i.e. magnetization is first transferred from A to B via physical coupling and then from B to C via chemical coupling [9,10].

Table 2
NMR parameters of complex **6b** [a,b]

Position number [c]	$^1H(\delta)$	$^{13}C(\delta)$	$J_{H,H}$(Hz)
1	8.65	151.37	$J_{1,2}=5.36$; $J_{1,3}=1.27$; $J_{1,4}=1.07$
2	7.48	127.72	$J_{2,3}=5.97$; $J_{2,4}=2.99$
3	7.89	140.39	$J_{3,4}=8.00$
4	7.91	122.67	
5		154.76	
6		153.19	
7	7.80	122.28	$J_{7,8}=8.08$; $J_{7,9}=1.43$; $J_{7,10}=1.00$
8	7.77	140.23	$J_{8,9}=7.46$; $J_{8,10}=1.62$
9	7.29	127.27	$J_{9,10}=5.25$
10	7.83	148.69	
11	–	118.24	
12	6.25	98.20	$J_{12,13}=6.93$; $J_{12,14}=1.1$
13	7.55	136.56	$J_{13,14}=7.66$
14	7.83	131.47	$J_{14,15}=7.45$; $J_{14,16}=1.1$
15	7.57	134.18	$J_{15,16}=7.96$
16	7.31	113.52	
17	3.55	56.72	$J_{17,18}=6.8$
18	1.30	14.43	

[a] Solvent, $CDCl_3$; [b] $[\{3,5\text{-}(CF_3)_2C_6H_3\}_4]^-$ (δ): ^1H, 7.62 (ortho H), 7.40 (para H); ^{13}C, 117.5 (para C), 124.5 (q, CF_3, $J_{CF}=268$ Hz), 129.2 (q, meta C, $J_{CF}=27$ Hz), 135.0 (ortho C), 161.5 (q, ipso C, $J_{CB}=50$); [c] atom labelling as in Fig. 1.

2.4. $[(\eta^3\text{-}syn\text{-}\alpha\text{-}methylbenzyl)Pd(dipy)]^+[B\{3,5\text{-}(CF_3)_2C_6H_3\}_4]^-$ (6b)

The NMR parameters are listed in Table 2. The average line width of resonances H12, H13, H15, and H16, is ca. 4 Hz. Such a relatively large value may be attributed to magnetic site exchange, slow on the chemicalshift timescale. Accordingly the 2D-NOESY spectrum (Fig. 2) has positive cross peaks H12/H16. Cross peaks H13/H15 are not observed owing to the extremely small chemical shift difference between these protons. An additional chemical exchange process is indicated by positive cross peaks H1/H10, H2/H9 and H3/H8.

The essential information of the NOESY negative correlations are summarized in Fig. 3, which contains

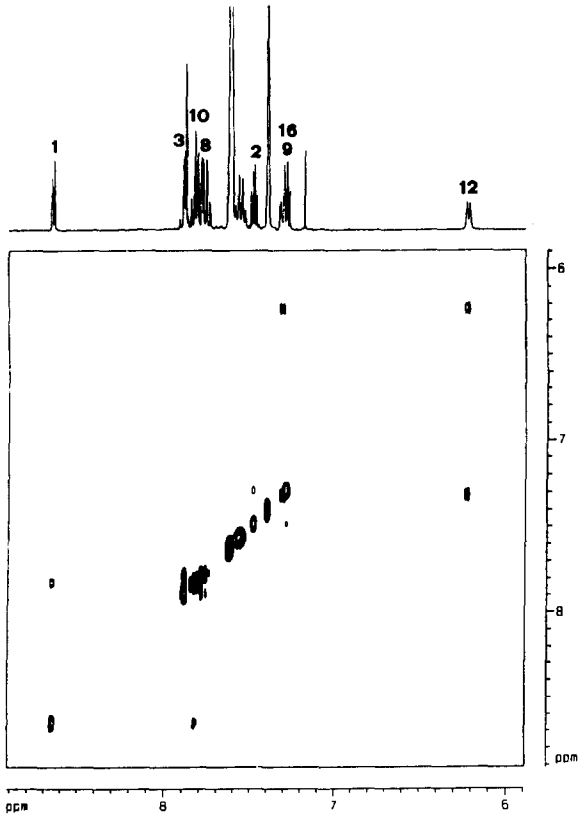

Fig. 2. 2D-NOESY spectrum of **6b**. Positive cross peaks.

the 1D spectrum compared with three columns of the 2D plot corresponding to the three well-resolved benzyl signals H12, H17, and Me18. The NOESY negative cross peaks between H12, H17, Me18 of the benzyl and H1, H10 of the bipyridyl protons can be used to define the arrangement of the ligands around the metal, employing the reporter ligand concept introduced by Pregosin [11–13]. The first column shows a cross peak H12/H10, suggesting that H12 and H10 interact across the metal. The strong correlation H12/H17 is due to the *anti-anti* allylic interaction. The H12/Me18 correlation may be attributed to indirect NOE, in the sense that Me18 transfers magnetization to H16 which in turn exchanges magnetic site with H12. The second portion of the 2D map shows the reporter cross peak H17/H1. The H17/Me18 and H17/H12 cross peaks are expected to be direct NOEs whereas the H17/H16 cross peak is again an indirect NOE, i.e. dipolar coupling between H12 and H17 in addition to chemical coupling between H12 and H16. Finally, in the third column cross peaks Me18/H1, Me18/H16, Me18/H17 are direct NOEs confirming the proximity of Me18, to H1, H16 and H17. Cross peak Me18/H12 is a transferred NOE due to H12/H16 chemical exchange, as discussed above. In conclusion, the above analysis of NMR data suggests that the structure of **6b** in solution is similar to the crystal structure and that dynamic equilibria are operative.

The NOESY exchange pattern may be rationalized on the basis of the following dynamic processes (Scheme 1).

(1) η^3-η^1 equilibrium of the coordinated benzyl group and simultaneous rotation of the benzyl group around the C11–C17 bond (Scheme 1, C_α–C_{ipso}).

(2) Exchange of the coordinated sites of the 2,2′-dipyridyl. The η^1-intermediate very likely has a T shape and allows exchange of the *ortho* protons H12/H16 (Scheme 1, H_α/H_β) by 180° rotation around the C11–C17 bond, leaving the 2,2′-dipyridyl in place. The coordination site exchange may take place through 180° rotation of a Y shape intermediate around the Pd–C bond a result there is H1/H10, H2/H9, H3/H8 exchange. In principle this exchange may also occur through ligand dissociation, but the results obtained with the TMEDA complex **4a** (vide infra) are consistent with the formation of a Y intermediate.

The rate constant k can be estimated from the ratio of the NOESY cross-peak intensity relative to that of the diagonal peak using the relation:

$$\frac{I_{\text{diag}}}{I_{\text{cross}}} \cong \frac{I - k\tau}{k\tau}$$

where τ is the mixing time [9]. Rotation around the C11–C17 bond seems slightly more favoured ($k = 9.5$

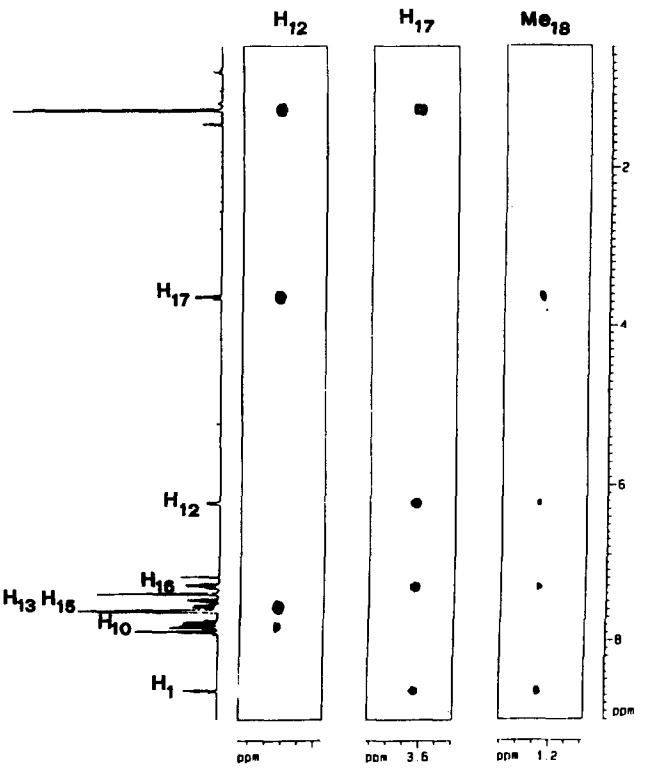

Fig. 3. 2D-NOESY spectrum of **6b**. Relevant negative cross peaks.

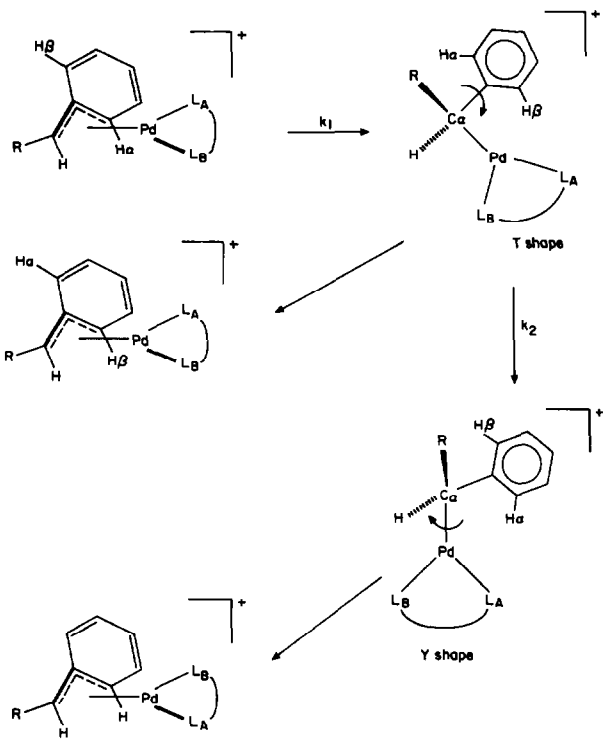

Scheme 1.

Table 3
NMR parameters of complex **4a** [a,b]

Position number [c]	$^1H(\delta)$	$^{13}C(\delta)$	$J_{H,H}$(Hz)
1	2.73	52.22	
2	2.46	49.52	
3a	2.30		$J_{3a,3b} = -13.8$; $J_{3a,4b} = 5.3$
		61.42	
3b	2.55		$J_{3b,4a} = 10.0$; $J_{3b,4b} = 3.6$
4a	2.19		
4		58.84	
4b	2.18		
5	1.86	48.1	
6	2.13	48.1	
11	–	117.35	
12	6.04	11.97	$J_{12,13} = 6.8$, $J_{12,14} = 1.1$
13	7.32	133.98	$J_{13,14} = 7.2$
14	7.66	130.70	$J_{14,15} = 7.8$, $J_{14,16} = 1.1$
15	7.38	133.48	$J_{15,16} = 7.9$
16	6.92	109.41	
17	3.08	62.52	$J_{17,18a} = 11.0$; $J_{17,18b} = 4.5$
18a	1.57		$J_{18a,18b} = -14.7$
18		22.80	
18b	1.48		
19	1.08	14.04	$J_{19,18} = 7.5$

[a] Solvent, $CDCl_3$; [b] anion parameters as reported in Table 2; [c] atom labelling as in Fig. 4.

s^{-1}, $\Delta G^* = 68 \pm 1$ kJ mol^{-1}, $T = 298$ K) than the rotation around the C17–Pd bond ($k = 0.3$ s^{-1}, $\Delta G^* = 77 \pm 1$ kJ mol^{-1}, $T = 298$ K). This is consistent with the slightly lower energy of the T intermediate with respect to the Y intermediate proposed by Hoffmann and coworkers [14,15].

2.5. *[(η^3-syn-α-ethylbenzyl)PdTMEDA]$^+$[B(3,5-(CF$_3$)$_2$-C$_6$H$_3$)$_4$]$^-$ (4a)*

The spectral parameters are reported in Table 3, the atom labelling in Fig. 4. The methyl resonances of TMEDA were assigned on the basis of NOE correlations. Me1 and Me6 have dipolar coupling with H17 and H12, respectively. Therefore Me1, Me6, H17 and H12 are on the same side of the coordination plane. Accordingly Me5 and Me2 show dipolar coupling with H13 and H18, respectively, which places Me5, Me2, H13 and H18 on the other side of the coordination plane.

The analysis of the four-spin system of the NCH_2CH_2N fragment results in four vicinal coupling constants two of the *gauche* type and two of the *anti* type. The H_{3b} resonance was assigned using the NOE coupling with Me1 and Me6; the remaining resonances were assigned from the coupling pattern resulting from the spectrum simulation. These observations are consistent with a conformational equilibrium of the fragment as sketched in the Newman projections A1 and A2 of Fig. 5. The experimental values of the coupling constants $J_{(3a-4b)}$ and $J_{(3b-4a)}$ are rationalized as the weighted average of the individual couplings of fast exchanging conformers A1 and A2 as follows:

$$xJ_t + (1-x)J_g = J_{(3b-4a)}$$

$$xJ_g + (1-x)J_t = J_{(3a-4b)}$$

where x is the molar fraction of conformer A1 and the constants J_t and J_g can be estimated from empirical rules to be 12.81 e 1.73 Hz, respectively [16]. The two above relations afford the values 0.69 and 0.67 for x. This compares with an analogous feature for a TMEDA Pt complex [17]. The staggered conformation of the

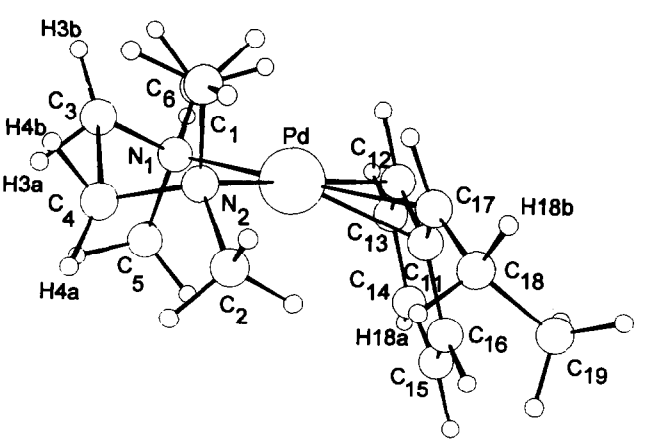

Fig. 4. A drawing of the cation [(η^3-syn-α-ethyllbenzyl)PdTMEDA]$^+$ in complex (**4a**).

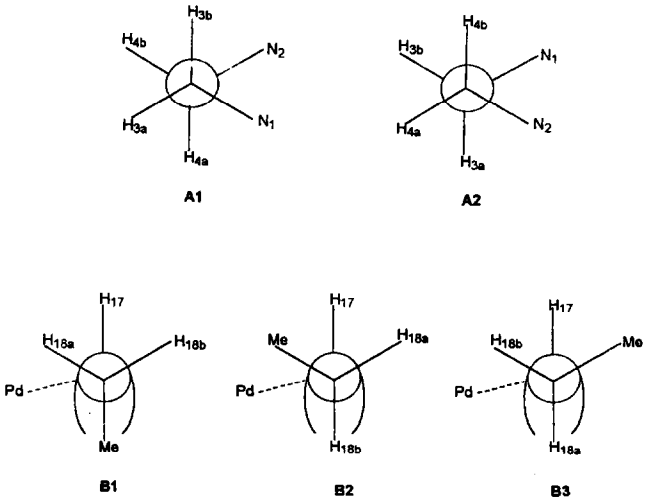

Fig. 5. (A) conformations of the **4a** PdTMEDA ring. (B) orientations of the methylene hydrogens of **4a** ethyl group.

NCH_2CH_2N fragment, consequent upon puckering of the five-membered $PdNCH_2CH_2N$ ring, has been previously observed in several X-ray structures [3,18]. Finally, inspection of the spectral parameters of the CH_3CH_2-benzyl fragment shows that the two diastereotopic methylene hydrogen atoms have markedly different vicinal coupling with H17, i.e. 4.5 and 11.0 Hz typical of a *gauche* and *anti* relationship respectively. This observation suggests that conformation B1 which shows two *gauche* relations is present in very low concentration and leaves B2 and B3 as predominant conformations (Fig. 5). Analogously to the spectrum of complex **6b** the 2D-NOESY spectrum shows positive cross peaks H12/H16 due to phenyl-ring rotation in the η^1 T intermediate and cross peaks Me1–Me5, Me2–Me6 (Fig. 6). The pairwise methyl exchange pattern of the TMEDA rules out the possibility of a ligand dissociation as it should produce random methyl exchange and suggests the rotation around the Pd–C bond in the η^1 Y intermediate (Scheme 1) as the most likely mechanism. The exchange rate constants at 298°C are 9.5 s^{-1} and 0.1 s^{-1}, respectively, for *ortho* hydrogens and TMEDA methyl exchange. Therefore **4a** has the same free energy barrier for exchange of the *ortho* protons as **6b** (68 ± 1 kJ mol^{-1}), which is slightly lower than that observed for the coordination-site exchange of the ligand (79 ± 1 kJ mol^{-1}). This result is also consistent with the slightly higher energy of the Y intermediate with respect to the T intermediate.

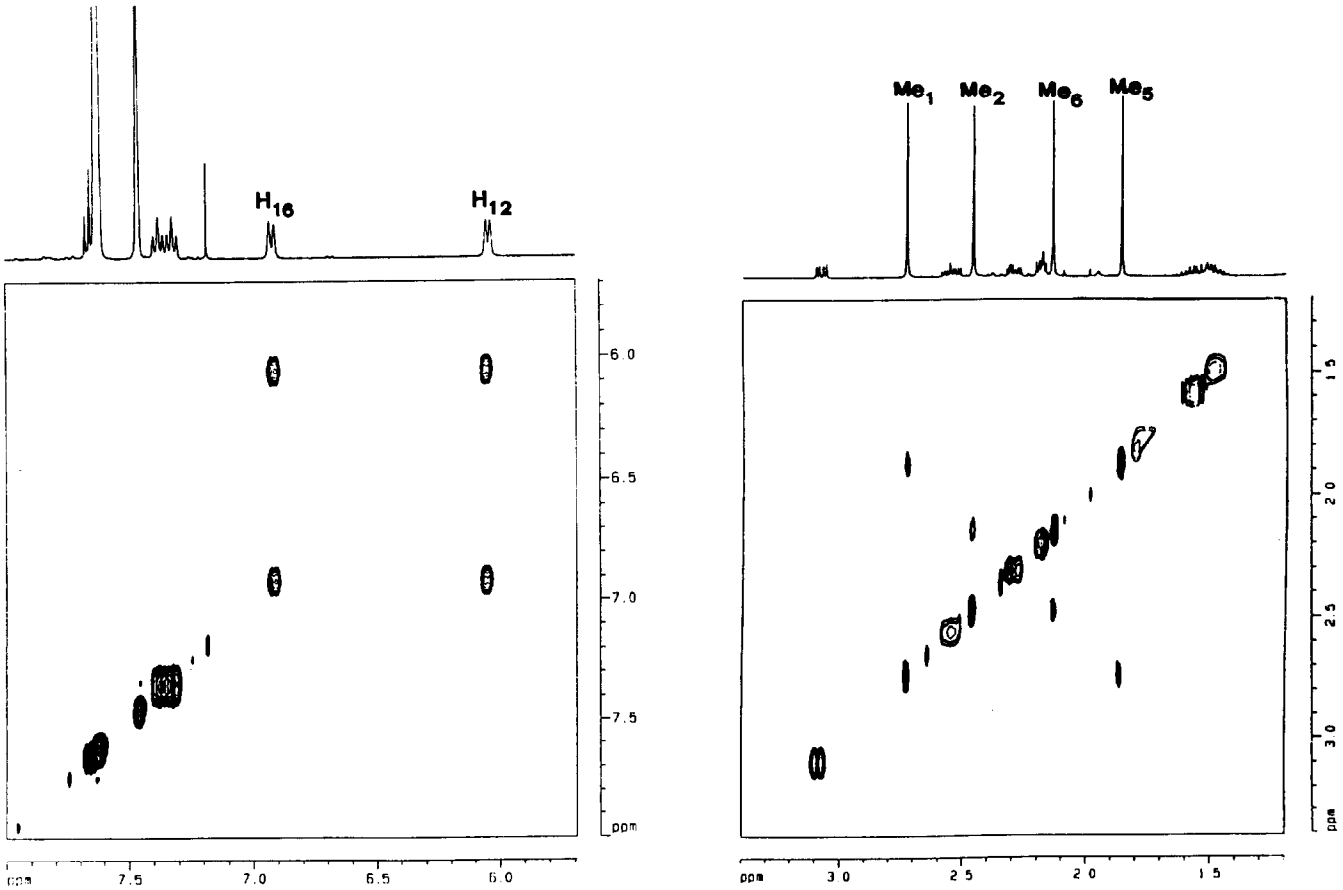

Fig. 6. 2D-NOESY spectrum of **4a**. Positive cross peaks.

Additional information may be derived from the 2D-NOESY spectrum, the essential features of which are collected in Fig. 7. The cross peak H12/H17 is the usual *anti–anti* interaction. The H12/H13 crosspeak is the expected *ortho* interaction. The correlations H12/H18, H12/Me19 are of indirect type, that is, transmitted through chemical exchange H12/H16. The pattern of column H16 is similar to that of column H12, a consequence of the rotation of the phenyl ring which exchanges the two sites. Me1 and Me2 interact differently with the diastereotoipic H18 protons. Whereas H18a interacts only with Me2, H18b has NOE contacts with both Me1 and Me2 suggesting an approximate equidistance from the methyl groups. The assignment of H18a is further confirmed by its proximity to H12 as shown by the pertinent NOE cross peak accompanied by the transferred NOE cross peak with H16. Finally it can be noted that the dipolar interaction of H17 with H18b is larger than that with H18a. This rules out conformation B2 and leaves B3 (Fig. 5) as the most probable conformation. Moreover conformation B3 implies that H18b is much closer to the metal than H18a. As a consequence the β-hydrogen elimination (Eq. (2)) should occur through migration of H18b to the Pd, which leaves H17 and H18a in a *trans* relationship, consistent with the observed formation of *E*-α-methylstyrene. In conclusion the NMR data indicate that the orientation of the benzyl group in **4a** relative to the Pd coordination plane is similar to that of **6b**.

2.6. $[(\eta^3\text{-syn-}\alpha\text{-ethylbenzyl})PdDPPP]^+[B\{3,5\text{-}(CF_3)_2C_6H_3\}_4]^+$ (4c) and $[(\eta^3\text{-syn-}\alpha\text{-methylbenzyl})PdDPPP]^-[B\{3,5\text{-}(CF_3)_2C_6H_3\}_4]^-$ (6c)

An exchange of the benzyl group similar to that observed for complexes **4a** and **6b** was monitored by the positive NOESY cross peaks relative to the *ortho* and *meta* protons of the phenyl ring. For both complexes the measured intensity of the cross peaks gives an exchange rate constant at room temperature similar to that observed for complexes **4a** and **6b**, therefore k_1 (Scheme 1) apparently does not depend on the particular ligand coordinated to the metal. On the other hand, the process relative to the exchange of the coordination sites was not observed for **4c** and **6c** within the limit of the sensitivity of the NOESY spectrum. An unusual high barrier to T–Y equilibrium has also been

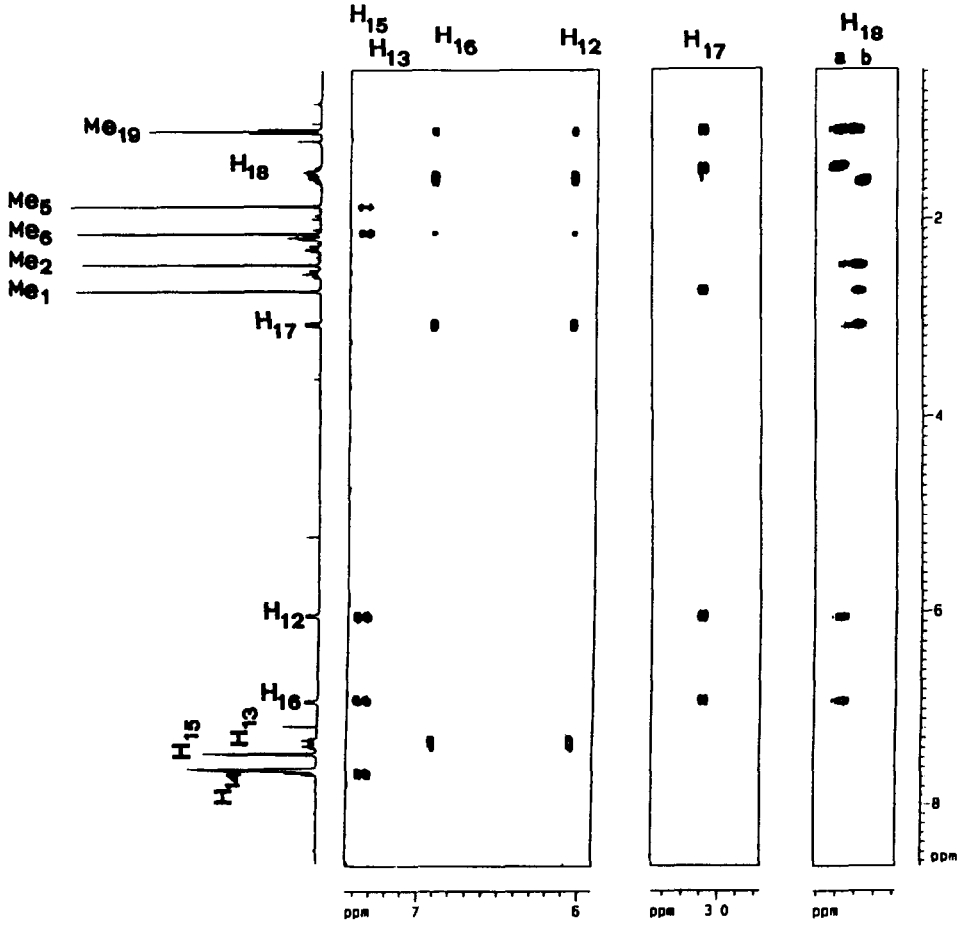

Fig. 7. 2D-NOESY spectrum of **4a**. Relevant negative cross peaks.

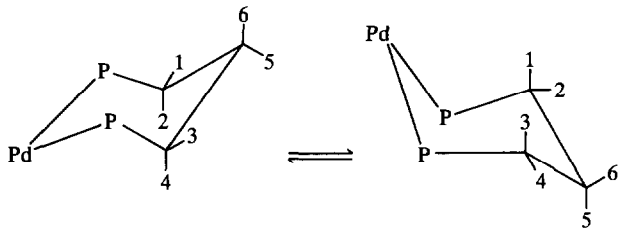

Fig. 8. Conformations of the PdDPPP ring in complexes **4c** and **6c**.

proposed by Spencer [19] for unsaturated ethyl (diphosphine)platinum cations.

The DPPP trimethylene fragment, which has the same chemical shifts and J pattern in both **4c** and **6c**, has been assigned through COSY experiments with broad decoupling by ^{31}P and spectrum simulation. The values of the vicinal coupling constants can be interpreted on the basis of a fast exchange between two chair conformations of the six-membered ring (Fig. 8). The values of the coupling constants $J_{1,6} = 2.1$ Hz, $J_{2,5} = 2.0$ Hz, $J_{2,5} = 2.0$ Hz, $J_{3,6} = 2.0$ Hz and $J_{4,5} = 2.4$ Hz, correspond to an equilibrium average value $J_{ae} \Leftrightarrow J_{ea}$. The observed low values, 2.0–2.5 Hz, as compared to the expected 4 Hz value [16] for a *gauche* coupling, suggest that the corresponding dihedral angle is smaller than 60°, i.e. there is some distortion of the ideal chair conformation [20]. The other two pairs of vicinal couplings $J_{1,5} = 8.9$ Hz and $J_{2,6} = 10.0$ Hz on one side, and $J_{3,5} = 8.7$ Hz and $J_{4,6} = 10.3$ Hz on the other side should correspond to the equilibrium average value $J_{aa} \Leftrightarrow J_{ee}$ which is estimated to be 8.8 Hz for a 1:1 ratio of the two chair conformations [16]. The observed values are indeed of this order of magnitude; the slightly higher values of two of them (10.0 and 10.3 Hz) may be attributed to a small difference between the molar fractions of the two chair conformations.

The ^{31}P spectra of **4c** and **6c** are AB quartets with very similar chemical shifts and J_{PP} values ($\delta \approx 17$ and ≈ 4, $J \approx 74$ Hz). The resonance at 17 δ is assigned to the phosphorus *cis* to the exocyclic benzyl carbon. The assignment derives from the proton spectra measured with selective decoupling of the phosphorus atoms.

The ^{13}C spectra are consistent with the proposed structures. The values of the chemical shifts compare well with those reported by Spencer [2] for $[(\eta^3\text{-MeCHPh})PdL_2]^+BF_4^-$ ($L_2 = Bu^t_2P(CH_2)_2PBu^t_2$, $Bu^t_2P(CH_2)_3PBu^t_2$, or $Bu^t_2P(CH_2C_6H_4CH_2PBu^t_2)$, although an *anti* stereochemistry has been proposed for these complexes on the basis of the ^1H-NMR chemical shits.

2.7. Reaction with carbon monoxide

The TMEDA complex **4a** reacts with carbon monoxide as shown by the ^{13}C-NMR spectrum of a $CDCl_3/CH_2Cl_2$ (1:1) solution saturated with carbon monoxide. As extensive decomposition to metallic palladium occurs on standing at room temperature, the ^{13}C data were collected at −30°C. The NMR data are consistent with formation of complex **7a** (Eq. (4)).

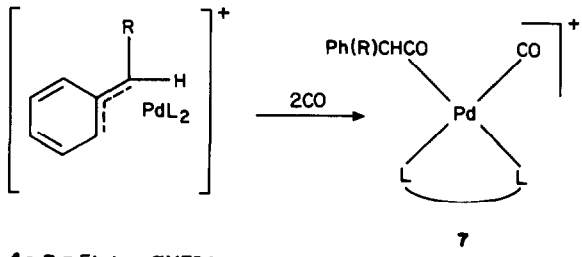

7

4a R = Et, L_2 = TMEDA

6b R = Me, L_2 = dipy

(4)

The values of the chemical shifts at 219.5 and 172.0 δ assignable to the inserted and coordinated carbon monoxide, respectively, compare with literature data [4,21–23]. Consistently the ^1H-NMR spectrum ($CDCl_3$, 25°C) shows a doublet of doublets at $\delta = 3.97$ ($J = 5.7$, 9.2 Hz) assignable to proton–COC*H*CH_2– coupled with diasteretopic CH_2 protons. The reaction with carbon monoxide is reversible. Compound **4a** is reformed on bubbling dinitrogen through the solution previously saturated with carbon monoxide, and therefore compound **7a** could not be isolated in a pure form.

The 2,2′-dipyridyl complex **6b** also reacts with carbon monoxide according to Eq. (4). At room temperature the ^1H NMR spectrum of a $CDCl_3$ solution saturated with carbon monoxide showed a quartet at 4.39 δ ($J = 6.7$ Hz) assignable to –COC*H*Me. However, in contrast to the TMEDA case, formation of **7b** is not quantitative at room temperature as compound **6b** is still present (**7b**:**6b** = 3:1). At −30°C compound **6b** disappears and only compound **7b** is present. Again, as observed for **7a**, bubbling dinitrogen through the $CDCl_3$ solution reforms compound **6b**.

The phosphine complex **4c** does not react with carbon monoxide under the reaction conditions under which **4a** and **6a** react. This experimental fact is not unprecedented. Insertion of CO in Pd–alkyl bond is fast if a nitrogen ligand is coordinated to the metal, slower in the case of a phosphorus ligand [24–27]

Preliminary results have shown that complex **6b** is a catalyst for copolymerization of CO and styrene to a syndiotactic polymer in either methanol or methylene chloride, which is expected in the light of a recent paper by Brookhart [4].

Complex **4a** has a different reactivity. In methanol it reacts quantitatively with carbon monoxide to yield methyl 2-phenyl butyrate and metallic palladium. Efforts are under way to make the above reaction catalytic, which would open a new route to 2-aryl alkanoates.

3. Conclusions

η^3-Benzyl Pd complexes may be prepared by reaction of $[Me_2PdL_2]$ (L_2 = TMEDA, DIPY) with tetrakis(3,5-bis(trifluoromethyl)phenyl)boric acid in presence of styrene. The TMEDA in the resulting η^3-*syn*-α-ethylbenzyl complex is easily displaced by a chelating phosphorus ligand such as DPPP. Such reactions should allow us to modulate the reactivity of the η^3-benzyl complex. Indeed we have now shown that the DIPY complex **6b** is a very active catalyst for the syndiotactic copolymerization of styrene and carbon monoxide at low carbon monoxide pressure and at low temperatures. The X-ray structure determination of complex **6b** has proved that the η^3-benzylic coordination is similar to that in other structures reported [3]. Finally a detailed NMR investigation has shown that the η^3–η^1 equilibrium of the coordinated benzyl group proceeds through a T-intermediate, and has offered a rationale for the stereospecific β-hydrogen elimination of *E*-1-methylstyrene from complexes **4**.

4. Experimental section

4.1. NMR measurements

High resolution NMR spectra were obtained on an AMX 400 MHz Bruker spectrometer equipped with a 5 mm multinuclear probe head for ^1H detection and inverse or direct detection of heteronuclei and provided with temperature control of the sample. The following typical acquisition and processing parameters were used.

^1H spectra

Pulse width 6.5 μs for 90°; spectral width 4000 Hz; data points 32 Kw zero filled to 64 Kw; relaxation delay 5 s; before Fourier transformation, time domain data were either sensitivity-enhanced by exponential multiplication in the case of accurate intensity measurements or resolution-enhanced by Lorentzian to Gaussian multiplication in the case of accurate multiplet analysis.

^{13}C spectra

Pulse width 11 μs for 90°; spectral width 20000 Hz; data points 64 Kw zero filled to 131 Kw; relaxation delay 2 s; before Fourier transformation time-domain data were sensitivity-enhanced by exponential multiplication.

^{31}P spectra

Pulse width 12 μs for 90°; spectral width 20000 Hz; data points 64 Kw zero filled to 131 Kw; relaxation delay 2 s; sensitivity enhancement by exponential multiplication.

2D-COSY spectra

Data table 1 Kw × 256 w, zero filled to 1 Kw; number of scans 16; dummy scans 4; relaxation delay 4 s; spectra acquired in second dimension in the phase sensitive mode TPPI, with doubler quantum filter; before Fourier transformation, time-domain data were multiplied in both dimensions by squared cosine window for sensitivity enhancement and apodization.

2D-NOESY spectra

Data table 1 Kw × 512 w, zerofilled to 1 Kw × 1 Kw; number of scans 32; dummy scans 4; relaxation delay 4s, mixing time 1 s for NOE and 10–50 ms for exchange; spectra acquired in second dimension in the phase-sensitive mode TPPI; squared cosine window; after phase correction the frequency domain spectra base line was smoothed in both dimension by polynomial correction.

2D ^1H-^{13}C inverse correlation

Pulse program: HMQC with BIRD saturation and GARP ^{13}C decoupling. Data table 1 Kw × 512 w, zerofilled to 1 Kw × 1 Kw; number of scans 64; dummy scans 16; relaxation delay 4 s; TPPI mode; square cosine window.

The measurements were performed on oxygen-free solutions in tubes sealed under vacuum. Similarly, the experiments with carbon monoxide-saturated solutions were performed in sealed tubes. $CDCl_3$ was purified by passage through a short column of neutral Al_2O_3.

4.2. Synthesis of the complexes

All the preparations were performed under dinitrogen. The solvents were dried by standard methods. The chemicals were Aldrich products. Styrene was distilled prior to use. $H[B(3,5\text{-}(CF_3)_2C_6H_3)_4]\cdot 2Et_2O$ was prepared according to Ref. [5], $[Me_2PdTMEDA]$ and $[Me_2PdDIPY]$ according to Ref. [3].

$[(\eta^3\text{-}syn\text{-}\alpha\text{-}ethylbenzyl)PdTMEDA]^+[B\{3,5\text{-}(CF_3)_2C_6H_3\}_4]^-$ (4a)

Styrene (2.08 g, 20 mmol) was added to $[Me_2PdTMEDA]$ (0.247 g, 0.98 mmol) dissolved in methylene chloride (6 ml). The resulting solution was magnetically stirred and cooled at −80°C. A cold methylene chloride (−80°C) solution of $H[B\{3,5\text{-}(CF_3)_2C_6H_3\}_4]\cdot 2Et_2O$ (1.00 g, 0.98 mmol) in methylene chloride (6 ml) was slowly siphoned into. The temperature was slowly raised (2 h) to −35°C. The solvent was then evaporated at reduced pressure keeping the temperature not higher than −30°C. The resulting orange oil was washed with hexane to yield **4a**

quantitatively as a yellow orange powder on scratching with a spatula. Analytically pure and crystalline samples can be obtained by slow diffusion at −30°C of hexane into a methylene chloride solution of **4a**. Analysis, calcd for $C_{47}H_{39}BF_{24}N_2Pd$: C 46.85; H 3.26; N 2.32; found: C 46.69; H 3.39; N 2.42%.

[(η^3-syn-α-methylbenzyl)PdTMEDA]$^+$[B{3,5-$(CF_3)_2C_6H_3$}$_4$]$^-$ (6a)

Complex **4a** (0.102 g, 0.085 mmol), styrene (0.208 g, 2 mmol) and H[B{3,5-$(CF_3)_2C_6H_3$}$_4$] · $2Et_2O$ (0.005 mg, 0.005 mmol) were dissolved in methylene chloride. The solution was kept in a tightly closed Schlenk tube at 55°C for 8 h. Small quantities of metallic palladium formed, which were separated by siphoning out the solution. The yellow–orange solution was concentrated (1 ml) and layered with hexane. At −30°C yellow–orange crystals (0.080 mg) of **6a** separated out. Analysis, calcd for $C_{46}H_{37}BF_{24}N_2Pd$: C 46.39; H 3.12; N 2.35; found C 46.52; H 3.20; N 2.44%.

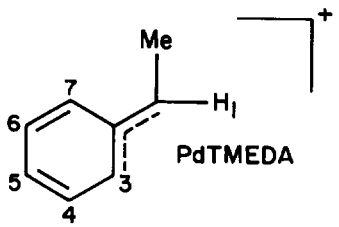

^{1}H-NMR ($CDCl_3$, δ): 1.10 (d, J = 6.7 Hz, 3H, Me); 1.88, 2.33, 2.51, 2.85 (s, 12H, N–Me); 2.2 ÷ 2.8 (m, 4H, $-NCH_2CH_2N-$); 3.14 (q, J = 6.7 Hz, 1H, H1); 5.96 (d, J = 7.0 Hz, 1H, H3); 7.15 (d, J = 8.3 Hz, 1H, H7); 7.44 (m, 2H, H6, H4); 7.7 (overlapping with anion resonances, H5).

[(η^3-syn-α-methylbenzyl)Pd(dipy)]$^+$[B{3,5-$(CF_3)_2C_6H_3$}$_4$]$^-$ (6b)

A cold (−80°C) methylene chloride solution (5 ml) of H[B{3,5-$(CF_3)_2C_6H_3$}$_4$] · $2Et_2O$ (0.425 g, 0.42 mmol) was added slowly to a cooled (−80°C) and magnetically stirred methylene chloride solution (4 ml) of [Me_2PdDIPY] (0.125 g; 0.42 mmol) and styrene (0.874 g; 8.4 mmol). The temperature was slowly raised to −10°C and kept overnight at that value. The reaction mixture was filtered through celite. Evaporation of the solvent left a yellow-brown oil which on scratching in hexane with a spatula yielded **6b** as a yellow powder quantitatively. Analytically pure and crystalline samples can be obtained by slow diffusion at −30°C of hexane into a methylene chloride solution of **6b**. Analysis calcd for $C_{50}H_{29}BF_{24}N_2Pd$: C 48.79; H 2.37; found C 46.93; H 2.44%.

[(η^3-syn-α-ethylbenzyl)PdDPPP]$^+$[B{3,5-$(CF_3)_2C_6H_3$}$_4$]$^-$ (4c)

$Ph_2P(CH_2)_3PPh_2$ (0.027 g, 0.066 mmol) and **4a** (0.080 g, 0.066 mmol) were dissolved in methylene chloride (1.5 ml). The resulting yellow solution was kept at room temperature for 0.5 h and then layered with hexane. **4c** was obtained as yellow crystalline material (0.075 g) through slow diffusion of hexane at −30°C. Analysis calcd for $C_{68}H_{49}BF_{24}P_2Pd$: C 54.40; H 3.29; found C 54.22; H 3.22%.

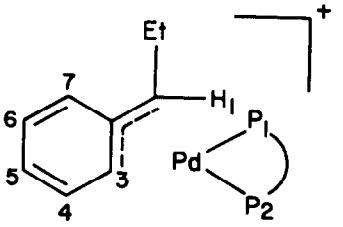

^{1}H-NMR ($CDCl_3$, δ, DPPP labelling as in Fig. 8): 0.64 (t, $J_{H,H}$ = 7.1 Hz, 3H, *Me*), 0.98–1.42 (m, 2H, CH_2Me), 1.80–1.63 (m, $J_{1,6}$ = 2.1 Hz, $J_{1,5}$ = 8.9 Hz, $J_{2,5}$ = 2.0 Hz, $J_{2,6}$ = 10.0 Hz, $J_{3,5}$ = 8.7 Hz, $J_{3,6}$ = 2.0 Hz, $J_{4,5}$ = 2.4 Hz, $J_{4,6}$ = 10.3 Hz, $J_{5,6}$ = −15.5 Hz, 2H, $CH_2CH_2CH_2$), 2.23–2.38–2.44–2.59 ($J_{1,2}$ = −15.0 Hz, $J_{3,4}$ = −15.3 Hz, 4H, $CH_2CH_2CH_2$), 3.42 (m, J_{H-H} = 11.4 Hz, J_{H-H} = 4.8 Hz, J_{H-P} = 9.9 Hz, 1H, H1), 6.39 (t, J_{H-H} = 7.8 Hz, J_{H-P} ≈ 7 Hz, 1H, H3), 6.59 (m, J_{H-H} = 7.5, J_{H-P} ≈ 7 Hz, 1H, H7), 6.83 (m, 1H, H5), 6.95 (m, 1H, H4), 7.06 (m, 1H, H6), 7.07 (m, 8H, *o*-Ph), 7.25–7.50 (m, 12H, m, *p*-Ph); ^{31}P-NMR ($CDCl_3$, δ): 4.2 (d, J_{P-P} = 73 Hz), 17.2 (d, J_{P-P} = 73 Hz).

Table 4
Summary of crystal data for [(η^3-*syn*-methylbenzyl)Pd(dipy)]$^+$[B{3,5-$(CF_3)_2C_6H_3$}$_4$]$^-$ (**6b**)

Formula	$C_{50}H_{27}BiF_{24}N_2Pd$
Mol. weight	1228.96
Crystal dimension, mm	0.1 × 0.15 × 0.15 mm^3
Crystal system	monoclinic
Space group	$P2_1/c$ (No. 14)
a, Å	13.823(3)
b, Å	15.645(3)
c, Å	24.515(9)
β, deg	104.10(2)
V, Å^3	5141.91
Z	4
ρ_{calc}, g cm^{-3}	1.59
μ(Cu-Kα), cm^{-1}	40.13
Radiation	graphite-monochromated Cu-Kα, λ = 1.5418 Å
Scan type	ω-2Θ
2Θ range, deg	5–120
Scan width, deg	1.2 + 0.34(tan Θ)
Scan speeds, deg s^{-1}	0.04–0.08
Total data	8189
Unique data, $I > 3(\sigma)$	4521
No. of refined parameters	516
R	0.098
R_w	0.110

Table 5
Atomic coordinates and thermal parameters of $[(\eta^3\text{-}syn\text{-}\alpha\text{-methylbenzylPddipy}]^+[B\{3,5\text{-}(CF_3)_2C_6H_3\}_4]^-$

Atom	x	y	z	U or U_{eq}
Pd1	1584(1)	1521(1)	1788(1)	76(1) [a]
N1	2468(9)	1125(10)	1269(6)	90(9) [a]
N2	2884(9)	1067(8)	2365(5)	73(7) [a]
C1	2215(14)	1160(15)	697(10)	127(15) [a]
C2	2788(16)	820(21)	381(11)	180(23) [a]
C3	3678(17)	455(19)	625(12)	167(22) [a]
C4	3968(14)	442(15)	1183(10)	126(16) [a]
C5	3363(11)	784(10)	154(8)	84(11) [a]
C6	3620(11)	802(9)	2124(7)	70(9) [a]
C7	4530(13)	577(11)	2465(11)	109(13) [a]
C8	4688(16)	586(12)	3015(10)	115(14) [a]
C9	3953(14)	845(11)	3252(9)	93(11) [a]
C10	3076(13)	1075(10)	2910(8)	83(11) [a]
C11	79(10)	1787(9)	1800(7)	68(9) [a]
C12	654(15)	2247(13)	2286(9)	105(13) [a]
C13	640(17)	1949(16)	2847(10)	116(16) [a]
C14	149(19)	1366(19)	2883(13)	152(21) [a]
C15	−416(18)	889(14)	2483(13)	144(18) [a]
C16	−445(155)	1122(12)	1927(11)	111(15) [a]
C17	267(13)	2008(16)	1283(8)	121(14) [a]
C18	−141(15)	1851(18)	780(9)	168(19) [a]
B1	7269(10)	3208(9)	−596(6)	46(3)
C1,1	6361(8)	2702(8)	−1046(5)	50(3)
C2,1	5474(8)	2446(8)	−911(5)	53(3)
C3,1	4700(10)	2071(9)	−1302(6)	62(3)
C4,1	4783(11)	1933(9)	−1842(6)	72(4)
C5,1	5631(10)	2213(9)	−1988(6)	68(4)
C6,1	6400(9)	2589(8)	−15580(5)	57(3)
C1,2	8363(8)	2910(7)	−658(5)	47(3)
C2,2	9213(9)	3416(8)	−473(55)	52(3)
C3,2	10147(9)	3182(8)	−487(5)	52(3)
C4,2	1031510)	2388(9)	−676(6)	68(4)
C5,2	9528(11)	1849(9)	−855(6)	69(4)
C6,2	8565(10)	2099(9)	−847(5)	64(4)
C1,3	7304(8)	3014(8)	58(5)	47(3)
C2,3	7687(9)	3553(8)	499(5)	55(3)
C3,3	7785(9)	3363(8)	1055(5)	57(3)
C4,3	7507(10)	2584(9)	1204(6)	66(4)
C5,3	7133(10)	1985(9)	798(6)	65(3)
C6,3	7055(9)	2188(8)	232(5)	60(3)
C1,4	7077(8)	4230(7)	−757(4)	41(3)
C2,4	6470(8)	4743(7)	−517(5)	49(3)
C3,4	6263(9)	5597(8)	−707(5)	58(3)
C4,4	6618(9)	5936(8)	−1130(5)	55(3)
C5,4	7209(9)	5406(8)	−1372(5)	54(3)
C6,4	7428(8)	4593(8)	−1191(5)	47(3)
C21	3759(14)	1786(13)	−1124(8)	95(5)
F1	3188(16)	2457(14)	−1083(10)	106(6)
F2	3977(16)	1394(14)	−634(10)	100(6)
F3	3347(17)	1125(15)	−1429(10)	112(6)
F1′	2965(13)	1745(12)	−1572(8)	87(5)
F2′	3916(21)	1002(19)	−906(14)	146(9)
F3′	3538(16)	2268(13)	−763(10)	103(6)
C22	5692(16)	2150(14)	−2598(8)	105(6)
F4	6075(14)	2813(12)	−2781(7)	87(5)
F5	6497(22)	1520(17)	−2581(11)	133(8)
F6	5066(20)	1562(16)	−2871(10)	118(7)
F4′	6523(25)	2343(24)	−2686(13)	161(10)
F5′	4872(15)	2409(13)	−2953(8)	104(6)
F6′	5723(30)	1333(19)	−2752(13)	145(10)
C23	11005(12)	3772(11)	−260(7)	82(4)
F7	11870(18)	3395(14)	−186(12)	116(7)
F8	10847(15)	4554(13)	−508(10)	105(6)
F9	11050(15)	4034(15)	277(9)	102(6)
F7′	11521(22)	3442(17)	240(12)	142(9)
F8′	11699(14)	3754(13)	−564(9)	97(6)
F9′	10872(16)	4484(16)	−86(12)	120(7)
C24	9675(20)	901(16)	−1082(11)	123(7)
F10	9029(17)	765(14)	−1518(10)	114(7)
F11	9634(23)	413(18)	−646(12)	151(9)
F12	10592(15)	854(12)	−1168(10)	99(6)
F10′	10464(20)	595(16)	−777(12)	133(8)
F11′	8997(17)	447(14)	−1115(10)	107(6)
F12′	9889(27)	1041(22)	−1578(15)	178(11)
C25	8253(14)	3992(12)	1486(8)	90(5)
F13	9129(15)	4296(14)	1419(9)	94(6)
F14	8514(15)	3649(12)	2018(8)	93(5)
F15	7646(22)	4549(19)	1535(12)	145(10)
F13′	9214(20)	3953(19)	1643(12)	133(9)
F14′	7893(18)	3972(15)	1957(9)	113(6)
F15′	7981(14)	4841(12)	1347(8)	92(6)
C26	6851(14)	1109(13)	937(9)	98(5)
F16 [b]	7521(12)	521(9)	859(6)	104(4)
F17 [b]	6730(13)	1035(10)	1444(7)	112(5)
F18 [b]	6003(11)	812(9)	570(6)	107(4)
F16′ [b]	5852(37)	1226(32)	960(22)	135(15)
F17′ [b]	6907(43)	568(33)	653(22)	117(15)
F18′ [b]	7262(32)	886(24)	1472(16)	85(11)
C27	5605(13)	6118(12)	−409(8)	86(5)
F19	5884(17)	6099(15)	120(10)	84(7)
F20	4637(17)	5742(16)	−558(10)	102(8)
F21	5504(16)	6916(13)	−628(9)	95(6)
F19′	5960(15)	6961(12)	−353(9)	89(6)
F20′	4681(16)	6101(16)	−714(9)	99(7)
F21′	5556(19)	5866(16)	90(11)	107(9)
C28	7585(13)	5713(11)	−1859(7)	85(5)
F22	8613(10)	5750(10)	−1704(7)	55(4)
F23	7268(15)	6442(13)	−2118(10)	87(6)
F24	7409(19)	5159(16)	−2311(10)	112(8)
F22′	8471(16)	5454(15)	−1898(9)	99(7)
F23′	7456(13)	6623(12)	−1890(8)	71(5)
F24′	7022(16)	5382(13)	−2333(8)	83(6)

Thermal parameters are multiplied by 10^3 and coordinates by 10^4.
[a] Atoms refined anisotropically. U_{eq} being defined as $\frac{1}{3}$ of the trace of the orthogonalized thermal tensor. All of the fluorine atoms were located and refined at distinctive positions (primed and unprimed symbols).
[b] The population parameters were all fixed at 0.5 with the exception of the atoms marked [b], the population parameters of the marked atoms are 0.75 (unprimed) and 0.25 (primed), respectively.

$[(\eta^3\text{-}syn\text{-}\alpha\text{-methylbenzyl})PdDPPP]^+[B\{3,5\text{-}(CF_3)_2C_6H_3\}_4]^-$ (6c)

$H[B\{3,5\text{-}(CF_3)_2C_6H_3\}_4]\cdot 2Et_2O$ (0.0022 g, 0.0021 mmol) was added to a chloroform solution (2 mL) of **4c** (0.065 g, 0.043 mmol) and styrene (0.045 g, 0.43 mmol). The resulting pale yellow solution was kept at 55°C overnight. The solvent was then removed in vacuum.

The oily residue was scratched with a spatula in hexane to yield **6c** as a cream colored powder. Analysis

calcd for $C_{67}H_{47}BF_{24}P_2Pd$: C 54.11; H 3.19; found C 53.97; H 3.37%.

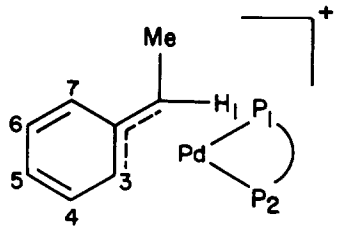

^{1}H-NMR ($CDCl_3$, δ): 0.91 (dt, $J = 6.7$ Hz, $J_{H-P} = 12.4$, 3H, *Me*), 3.38 (m, $J_{H-H} = 6.7$ Hz, $J_{H-P} = 8.9$ Hz, 1H, H1) 6.18 (t, $J_{H-H} = 6.8$ Hz, $J_{H-P} \approx 7$ Hz, 1H, H3), 6.79 (m, 1H, H7), 6.83 (H5, partially overlapping with phenyl protons), 6.84 (H4, overlapping with phenyl protons), 7.15 (m, 1H, H6), DPPP chemical shifts and J as in **4c**; ^{31}P-NMR ($CDCl_3$, δ): 4.2 (d, $J_{P-P} = 74$ Hz), 17.0 (d, $J_{P-P} = 74$ Hz).

4.3. X-ray structure determination of [(η^3-syn-α-methylbenzyl)Pd(dipy)]$^+$[B{3,5-(CF_3)$_2$$C_6H_3$}$_4$]$^-$ (6c)

A pale yellow cubic crystal was selected for X-ray analysis. Crystal data were collected on a Philips PW1100 diffractometer governed by a new operating system (FEBO [28]). A set of 25 carefully centred reflections having $13.5 < \theta < 15°$ were used to determine the cell constants. As general procedure, three standard reflections were measured every 2 h for orientation and intensity control. No decay of the specimen was noticed. Intensity data were corrected for Lorentz-polarization effects. Atomic scattering factors were those reported by Cromer and Waber [29] with anomalous dispersion correction. An empirical absorption correction was applied via ψ scan measurements with transmission factors in the range 1.35–1.0. All the computational work was carried out on a Digital Dec 5000/200 workstation using the programs SHELX76 [30] and SHELX86 [31]. The programs PARST [32] and PLUTO [33] were also used. Crystallographic details are reported in Table 4. Final atomic coordinates with equivalent isotropic thermal parameters are reported in Table 5. The structure was solved by using the heavy atom technique and all of the non-hydrogen atoms were found through a series of F_0 Fourier maps. No hydrogen atom could be located and they were introduced at a later stage in calculated positions but not refined. The H atoms attached to the metal-coordinated allyl carbon atoms have not been introduced. Refinement was by full-matrix least square calculations, initially with isotropic thermal parameters. In the last L.S. cycles, anisotropic thermal parameters were used for all of the non-hydrogen atoms in the complex cation but not for those in the anion [B(3,5-(CF_3)$_2$$C_6H_3$)$_4$]$^-$. In the latter, all the CF_3 groups are clearly affected by rotational disorder about the C–C(F_3) linkages to the C_6 ring. Two preferred positions could be assigned to the F atoms of each CF_3 group. All of the fluorine population parameters were fixed at 0.5 with the exception of the atoms F16-F18 (F'16-F'18) whose temperature factors behave better with population parameters of 0.75 and 0.25, respectively. Unfortunatley, even such a complicated description of the CF_3 groups does not fully account for the residual electron density, as large as 1.1 eÅ^{-3} in some parts of the final ΔF map. Certainly, this problem contributes to the unusually high R factors ($R = 0.098$ and $R_w = 0.110$) and to the large atomic standard deviations at the end of the refinement. Working with a different set of data collected from another crystal led to the same poor crystallographic results. Listings of atomic coordinates of the hydrogen atoms, anisotropic thermal parameters have been deposited with the Cambridge Crystallographic Data Centre, and these listings and structure factors are also available from the authors.

Acknowledgements

The research has been supported by the Progetto Finalizzato CNR, Chimica Fine II and the MURST. The work of Dr. J.A. López, c/o ISSECC has been made possible through a grant of the Ministerio de Educación y Ciencia of the Spanish Government.

References

[1] Leading references: J. Sholz, F. Rehbaum, K.H. Thiele, R. Goddard, P. Betz and C. Krüger, *J. Organomet. Chem., 443* (1993) 93; N.H. Dryden, P. Legzdins, J. Trotter and V.C. Yee, *Organometallics, 10* (1991) 2857; recent works include D.J. Growther, S.L. Borkowsky, D. Swenson, T.Y. Meyer and R.F. Jordan, *Organometallics, 12* (1993) 2897; C. Pellecchia, A. Immirizi, A. Grassi and A. Zambelli, *Organometallics, 12* (1993) 4473.

[2] Co: E.L. Muetterties and F.J. Hirsekorn, *J. Am. Chem. Soc., 96* (1974) 7920; J.R. Bleeke, R.R. Burch, C.L. Coulman and B.C. Schardt, *Inorg. Chem., 20* (1981) 1316; V. Galamb and G. Pályi, *J. Chem. Soc., Chem. Commun.*, (1982) 487. Rh: H.O. Stühler, *Angew. Chem., Int. Ed. Engl., 19* (1980) 468; H.O. Stühler and J. Pickardt, *Z. Naturforsch. Teil B., 36* (1981) 315; S.D. Chappel, D.J. Cole-Hamilton, A.M.R. Galas, M.B. Hursthouse and N.P.C. Walker, *Polyhedron, 4* (1985) 121; B. Ebbinghaus, M.T. Madigan, C.E. Osterberg and L.C. Nathan, *Acta Crysrtallogr., C44* (1988) 21; M.D. Fryzuk, D.H. McConville and S.J. Rettig, *J. Organomet. Chem., 445* (1993) 245. Ni: J.R. Ascenso, A.R. Dias, P.T. Gomes, C.C. Romão, Q.T. Pham, D. Neibecker and I. Tkatchenko, *Macromolecules, 22* (1989) 998; J. Cámpora, E.Gutiérrez, M.L. Poveda, C. Ruiz and E. Carmona, *J. Chem. Soc., Dalton Trans.*, (1992) 1769; J. Cámpora, E. Carmona, E. Gutiérrez, P. Palma, M.L. Poveda and C. Ruiz, *Organometallics, 11* (1992) 11. Pd: R.R. Stevens and G.D. Shier, *J. Organomet. Chem., 21* (1970) 495; J.S. Roberts and K.J. Klabunde, *J. Organomet. Chem., 85* (1975) C13; J.S. Roberts and K.J. Klabunde, *J. Am. Chem. Soc., 99* (1977) 2509; Y. Becker and J.K. Stille, *J. Am. Chem. Soc., 100* (1978) 845; B.E. Mann, A. Keasey, A. Sonoda and P.M. Maitlis, *J. Chem. Soc., Dalton*

Trans., (1978) 338; G.A. Rizzi, F. Morandini, A. Turco and F. Bergamin, *Gazz. Chim. Ital., 123* (1993) 359. Pt: L.E. Crascall, S.A. Litster, A.D. Redhouse and J.L. Spencer, *J. Organomet. Chem.*, 394 (1990) C35; L.E. Crascall and J.L. Spencer, *J. Chem. Soc., Dalton Trans.*, (1992) 3445.

[3] W. de Graaf, J. Boersma, W.J.J. Smeets, A.L. Spek and G. van Koten, *Organometallics, 8* (1989) 2907.

[4] M. Brookhart, F.C. Rix and J.M. DeSimone, *J. Am. Chem. Soc., 114* (1992) 5894.

[5] M. Brookhart, B. Grant and A.F. Volpe, Jr, *Organometallics, 11* (1992) 3920.

[6] R. Taube and S. Wache, *J. Organomet. Chem., 428* (1992) 431.

[7] C. Carfagna, R. Galarini, K. Linn, J.A. López, C. Mealli and A. Musco, *Organometallics, 12* (1993) 3019.

[8] R. Goddard, C. Krüger, F. Mark, R. Stansfield and X. Zhang, *Organometallics, 4* (1985) 285.

[9] R.R. Ernst, G. Bodenhausen and A. Wokaaun, *Principles of Nuclear Magnetic Resonance in One and Two Dimensions*, Clarendon, Oxford, 1987, pp. 490–538.

[10] D. Neuhaus, M.P. Williamson, *The Nuclear Overhauser Effect in Structural and Conformational Analysis*, VCH, New York, 1989, pp. 141–181.

[11] A. Albinati, C. Ammann, P.S. Pregosin and H. Rüegger, *Organometallics, 9* (1990) 1826.

[12] A. Togni, G. Rihs, P.S. Pregosin and C. Ammann, *Helv. Chim. Acta, 73* (1990) 723.

[13] A. Albinati, R.W. Kunz, C.J. Ammann and P.S. Pregosin, *Organometallics, 10* (1991) 1800.

[14] S. Komiya, T.A. Albright, R. Hoffmann and J.K. Kochi, *J. Am. Chem. Soc., 98* (1976) 7255.

[15] K. Tatsumi, R. Hoffmann, A. Yamamoto and J.K. Stille, *Bull. Chem. Soc. Jpn., 54* (1981) 1857.

[16] R.J. Abraham and G. Gatti, *J. Chem. Soc. B*, (1969) 961.

[17] G. Frommer, F. Lianza, A. Albinati and B. Lippert, *Inorg. Chem., 31* (1992) 2434.

[18] R. Amstutz, T. Laube, W.B. Schweizer, D. Seebach and J.D. Dunitz, *Helv. Chim. Acta, 67* (1984) 224.

[19] L. Mole, J.L. Spencer, N. Carr and A.G. Orpen, *Organometallics, 10* (1991) 49.

[20] W.L. Steffer and G.J. Palenik, *Inorg. Chem., 15* (1976) 2432.

[21] J.S. Brumbaugh and A. Sen, *J. Am. Chem. Soc., 110* (1988) 803.

[22] M. Grassi, S.V. Meille, A. Musco, R. Pontellini and A. Sironi, *J. Chem. Soc., Dalton Trans.*, (1989) 615.

[23] Imre Tóth and Cornelius J. Elsevier, *J. Am. Chem. Soc., 115* (1993) 10388.

[24] G.P.C.M. Dekker, A. Buijs, C.J. Elsevier, K. Vrieze, P.W.N.M. van Leeuwen, W.J.J. Smeets, A.L. Spek, Y.F. Wang and C.H. Stam, *Organometallics, 11* (1992) 1937.

[25] G.P.C.M. Dekker, C.J. Elsevier, K. Vrieze and P.W.N.M. van Leeuwen, *Organometallics, 11* (1992) 1598.

[26] W. de Graaf, J. Boersma and G. van Koten, *Organometallics, 9* (1990) 1479.

[27] R.E. Rülke, I.M. Han, C.J. Elsevier, K. Vrieze, P.W.N.M. van Leeuwen, C.F. Roobeek, M.C. Zoutberg, Y.F. Wang and C.H. Stam, *Inorg. Chim. Acta, 169* (1990) 5.

[28] FEBO System, Pavia, Italy

[29] D.T. Cromer and J.T. Waber, *Acta Crystallogr., 18* (1965) 104.

[30] G.M. Sheldrick, SHELX76, *A Program for Crystal Structure Determination*, University of Cambridge, 1976.

[31] G.M. Sheldrick, SHELX87, *Structure Solving Program*, University of Gottingen, FDR, 1986.

[32] M. Nardelli, *Compt. Chem., 7* (1983) 95.

[33] W.D.S. Motherwell, PLUTO, *Plotting Program for Molecular Structure*, University of Cambridge, 1978.